

Galactic Chemical Evolution of the *s* Process from AGB Stars

Alessandra Serminato^{A,D}, Roberto Gallino^A, Claudia Travaglio^B,
Sara Bisterzo^A, and Oscar Straniero^C

^A Dipartimento di Fisica Generale, Università di Torino, via P. Giuria, 1, 10125 Torino, Italy

^B Osservatorio Astronomico di Torino (INAF), Strada Osservatorio 20, 10025 Pino Torinese, Italy

^C Osservatorio Astronomico di Collurania (INAF), via M. Maggini, Teramo 64100, Italy

^D Corresponding author. Email: ale.wicked.elf@gmail.com

Received 2008 November 25, accepted 2009 August 5

Abstract: We follow the chemical evolution of the Galaxy for the *s* elements using a Galactic chemical evolution (GCE) model, as already discussed by Travaglio et al. (1999, 2001, 2004), with a full updated network and refined asymptotic giant branch (AGB) models. Calculations of the *s* contribution to each isotope at the epoch of the formation of the solar system is determined by following the GCE contribution by AGB stars only. Then, using the *r*-process residual method we determine for each isotope their solar system *r*-process fraction, and recalculate the GCE contribution of heavy elements accounting for both the *s* and *r* process. We compare our results with spectroscopic abundances at various metallicities of [Sr,Y,Zr/Fe], of [Ba,La/Fe], of [Pb/Fe], typical of the three *s*-process peaks, as well as of [Eu/Fe], which in turn is a typical *r*-process element. Analysis of the various uncertainties involved in these calculations are discussed.

Keywords: nuclear reactions, nucleosynthesis, abundances — stars: AGB and post-AGB

1 Introduction

According to the classical analysis of the *s* process, the abundance distribution in the solar system was early recognized as the combination of three components (Clayton & Rassbach 1977; Käppeler et al. 1982): the main component, accounting for *s*-process isotopes in the range from $A \sim 90$ to $A < 208$, the weak component, accounting for *s*-process isotopes up to $A \sim 90$, and the strong component, introduced to reproduce about 50% of double-magic ^{208}Pb . The main component itself cannot be interpreted as the result of a single neutron exposure, but as a multi-component, like an exponential distribution of neutron exposures. It is clear that the *s* process does not originate in a unique astrophysical environment.

In this paper we study the Galactic chemical evolution of the *s* process as the outcome of nucleosynthesis occurring in low- to intermediate-mass AGB stars of various metallicities. These calculations have been performed with an updated network of neutron capture cross sections and β -decay rates. The paper is organized as follows: in Section 2 we briefly introduce the stellar evolutionary model FRANEC and the post-process network we use to compute the nucleosynthesis in AGB stars. In Section 3 we introduce the GCE model adopted. In Section 4 we present *s*-element contributions at the solar system formation by introducing in the GCE code the AGB *s* yields only obtained at various metallicities. The corresponding *r*-process contribution to solar abundances are then deduced with the *r*-process residual method. We recalculate with the GCE model the global *s+r* contribution

to the Galactic chemical evolution of heavy elements as a function of [Fe/H]. Our predictions are compared with spectroscopic data of Sr, Y, Zr, characterising the first *s* peak (light *s*, ls), of Ba and La, characterising the second *s* peak (heavy *s*, hs), and Pb at the third *s*-process peak, together with Eu, an element of most *r*-process origin. Finally, in Section 5 we summarise the main conclusions and point out few aspects deserving further analysis.

2 FRANEC and *s* Yields

The FRANEC (Frascati Raphson Newton Evolutionary code, Chieffi & Straniero 1999) self-consistently reproduce the third dredge up episodes in AGB stars and the consequent recurrent mixing of freshly synthesised *s*-processed material (together with ^4He and ^{12}C) with the surface of the star. Nucleosynthesis in AGB stars of different masses and metallicities is followed with a post-process code, which uses the pulse by pulse results of the FRANEC code: the mass of the He intershell, the mass involved in the third dredge up (TDU), the envelope mass that is progressively lost by intense stellar winds, the temporal behaviour of the temperature and density in the various layers of the zones where nucleosynthesis takes place. For numerical details on the key parameters affecting the *s*-process nucleosynthesis in AGB stars of low mass we refer to Straniero et al. (2003).

The network contains more than 1400 isotopes and is sufficiently extended to take into account all possible branchings that play a role in the nucleosynthesis process. The neutron capture network is updated with the

recommended (n,γ) rates by Bao et al. (2000), complemented by a series of more recent experimental results (for more details see Bisterzo et al. 2006). Stellar β decays are treated following Takahashi & Yokoi (1987). The production of *s*-process elements in AGB stars proceeds from the combined operation of two neutron sources: the dominant reaction $^{13}\text{C}(\alpha,n)^{16}\text{O}$, which releases neutrons in radiative conditions during the interpulse phase, and the reaction $^{22}\text{Ne}(\alpha,n)^{25}\text{Mg}$, marginally activated during thermal instabilities. In the model, the dominant neutron source is not based on physical principles (Gallino et al. 1998): during TDU, a small amount of hydrogen from the envelope may penetrate into ^{12}C -rich and ^4He -rich (He-intershell) inner zone. Then, at H-shell reignition, a thin ^{13}C -pocket may form in the top layers of the He-intershell, by proton capture on the abundant ^{12}C . We artificially introduce a ^{13}C pocket, which is treated as a free parameter. The total mass of the ^{13}C pocket is kept constant with pulse number and the concentration of ^{13}C in the pocket is varied in a large range, from values 0.005–0.08 up to 2 times with respect to the profile indicated as ST by Gallino et al. (1998), corresponding to the choice of the mass of ^{13}C of $3.1 \times 10^{-6} \text{ M}_\odot$. A too high proton concentration would favour the production of ^{14}N by proton capture on ^{13}C . Note that the minimum ^{13}C -pocket efficiency decreases with metallicity, since the neutron exposure depends on the ratio of the neutrons released to Fe seeds. This choice was shown to better reproduce the main component with AGB models of half-solar metallicity (Arlandini et al. 1999), and is a first approach to the understanding of solar system *s*-process abundances. In reality, the solar system composition is the outcome of all previous generations of AGB stars having polluted the interstellar medium up to the moment of condensation of the solar system. A spread of ^{13}C -pocket efficiencies has been shown to reproduce observations of *s*-enhanced stars at different metallicities (see, e.g. Busso, Gallino & Wasserburg 1999; Busso et al. 2001; Sneden, Cowan & Gallino 2008).

In AGB stars of intermediate mass the *s* process is less efficient. As for the choice of the ^{13}C neutron source, because of the much shorter interpulse phases in these stars (~ 650 yr for 5 M_\odot and ~ 1500 yr for 7 M_\odot) with respect to low-mass AGBs ($\sim 3\text{--}6 \times 10^4$ yr), the He intershell mass involved is smaller by one order of magnitude. Consequently, also the TDU of *s*-rich material from the He-intershell into the surface is reduced, again by roughly one order of magnitude. Given the above reasons, for the 5-M_\odot and the 7-M_\odot cases, as in Travaglio et al. (1999, 2004), we have considered as a standard choice for IMS-AGBs (ST-IMS) a ^{13}C mass scaled accordingly [$M(^{13}\text{C})_{\text{ST-IMS}} = 10^{-7} \text{ M}_\odot$]. On the other hand, in IMS stars the $^{22}\text{Ne}(\alpha,n)^{25}\text{Mg}$ reaction is activated more efficiently (Iben 1975; Truran & Iben 1977) since the temperature at the base of the convective pulse reaches values of $T = 3.5 \times 10^8$ K. Also, the peak neutron density during the TP phase is consistently higher than in AGBs ($N_n \sim 10^{11}$ neutrons cm^{-3} , see Vaglio et al. 1999;

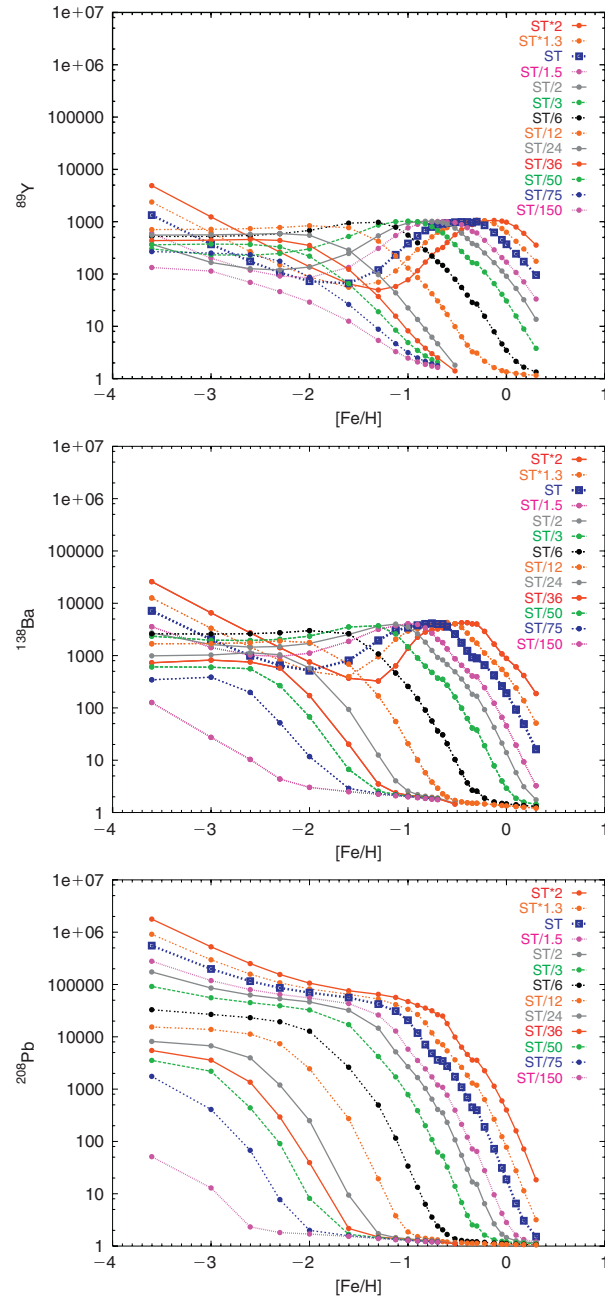


Figure 1 Top panel: theoretical prediction for ^{89}Y production factors versus metallicity using AGB models with initial mass $M = 1.5 \text{ M}_\odot$. Middle and bottom panel: analogous plots for ^{138}Ba and for ^{208}Pb .

Straniero et al. 2001), overfeeding a few neutron-rich isotopes involved in important branchings along the *s*-process path, such as ^{86}Kr , ^{87}Rb , and ^{96}Zr .

We took a set of low-mass stars (LMS, 1.5 to 3 M_\odot) and intermediate-mass stars (IMS, 5 to 7 M_\odot), and a set of 27 metallicities from $[\text{Fe}/\text{H}] = 0.30$ down to $[\text{Fe}/\text{H}] = -3.60$.

2.1 *s* Yields

In Figure 1 we show the theoretical predictions versus $[\text{Fe}/\text{H}]$, for AGB stars of initial mass $M = 1.5 \text{ M}_\odot$, of the production factors in the astroted *s*-process ejecta

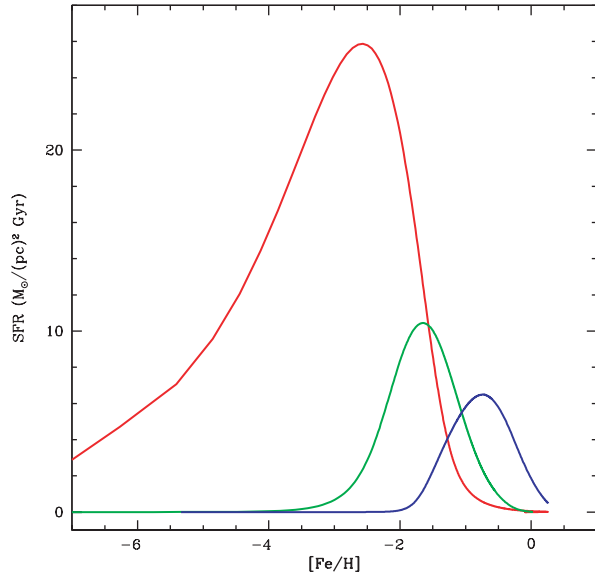


Figure 2 Star-formation rate versus metallicity.

of ^{89}Y , ^{138}Ba , and ^{208}Pb , taken as representative of the three *s*-process peaks. Each line corresponds to a given ^{13}C -pocket efficiency. The production factors are given in terms of the isotope abundance divided by the initial abundance, solar-scaled with metallicity. For low neutrons/seed ratios, the neutron fluence mainly feeds the ls nuclei (like ^{89}Y), whereas for higher exposures the hs peak (like ^{138}Ba) is favoured. Increasing further the neutron exposure, the neutron flow tends to overcome the first two *s* peaks, directly feeding ^{208}Pb at the termination point of the *s*-process path. There is therefore a very complex *s*-process dependence on metallicity.

3 The GCE Model

The model for the chemical evolution of the Galaxy was described in detail by Ferrini et al. (1992) and it was updated by Travaglio et al. (1999, 2001, 2004). The Galaxy is divided into three zones, halo, thick disc, and thin disc, whose composition of stars, gas (atomic and molecular), and stellar remnants is computed as function of time up to the present epoch $t_{\text{Gal}} = 13$ Gyr. Stars are born with an initial composition equal to the composition of the gas from which they formed. The formation of the Sun takes place 4.5 Gyr ago, at epoch $t_{\odot} = 8.5$ Gyr. The matter in the Galactic system has different phases of aggregation, interacting and interchanging one into the other. Therefore the evolution of the system (the time dependence of the total mass fraction in each phase and the chemical abundances in the ISM and in stars) is determined by the interaction between these phases. It means that the star formation rate (SFR, see Figure 2), $\psi(t)$, is not assumed *a priori*, but is obtained as the result of a self-regulating process occurring in the molecular gas phase, either spontaneous or simulated by the presence of other stars. The thin disc is divided into concentric annuli, without any radial flow, and is formed from material infalling from the thick and

the halo. In the present work, as in Travaglio et al. previous works, we neglect any dependence on Galactocentric radius in the model results as well as in the observational data and we concentrate on the evolution inside the solar annulus, located at 8.5 kpc from the Galactic center.

However, we must point out that the Galactic chemical evolution model by Ferrini et al. (1992) that we use is now believed to be incorrect. The main problem is that the thick disk cannot form from gas from the halo, as demonstrated by Wyse & Gilmore (1992). These authors showed that the distribution of angular momentum of halo stars differs markedly from that of the thick and thin disks. Pardi, Ferrini & Matteucci (1995) also demonstrated that the scenario we assume cannot reproduce at the same time the stellar metallicity distributions of the halo, thick disk, and thin disk. See also Pagel (1997) and Matteucci (2003). To overcome the problems of the model by Ferrini et al. (1992), Cescutti et al. (2006) studied the chemical evolution of the heavy elements using the two-infall model proposed by Chiappini, Matteucci & Gratton (1997). Also this model, although widely adopted, presents some shortcomings, for example, it is not possible to distinguish the thick disk from the thin disk. In the present paper we focus on analysing the changes made by using updated reaction rates on the chemical evolution of the elements heavier than iron rather than the changes made by using an updated model of the evolution of the Galaxy. Thus, we use the same model of Travaglio et al. (1999, 2001, 2004) where we introduce a new and extended grid of AGB yields. However, most of the uncertainties related to the GCE model are resolved by the fact that we normalise our abundances at the time and place of the solar system formation to the abundance of the *s*-only ^{150}Sm , so we are considering relative rather than absolute abundances.

4 Results for GCE of *s* and *r* Elements

In this section we present the results for the evolution of Sr, Y, Zr, La, Ba, Eu, and Pb in the Galaxy, by considering separately the *s* and *r* contributions. Then we compute the Galactic abundances of these elements resulting from the sum of the two processes, comparing model results with the available spectroscopic observations of field stars at different metallicities.

4.1 GCE of *s* Elements

The *s* contribution to each isotope at the epoch of the formation of the solar system is determined by following the GCE heavy elements contributed by AGB stars only. Then, using the *r*-process residual method ($s = 1 - r$) we determined for each isotope the solar system *r*-process fraction. As a second step, we recalculate the GCE contribution of the heavy elements accounting for both the *s* and the *r* process, assuming that the production of *r* nuclei is a primary process occurring in Type II supernovae, independent of the metallicity.

Galactic chemical *s*-process expectations depend on several uncertainties, among which are the knowledge of solar abundances, of the neutron capture network and on

Table 1. Contributions from stars at $t=t_{\odot}=8.5$ Gyr, as percentages to solar abundance

Isotope	Travaglio (1999)	This work
LMS-AGB ^a (% to solar)		
⁸⁹ Y	61.5	62.7
¹²⁴ Te	72.0	70.0
¹³⁶ Ba	92.1	85.1
¹³⁸ Ba	84.0	82.3
¹³⁹ La	61.4	65.5
¹⁵⁰ Sm	98.1	99.1
¹⁵¹ Eu	6.4	5.7
²⁰⁴ Pb	93.8	85.1
²⁰⁸ Pb	93.6	90.7
IMS-AGB ^b (% to solar)		
⁸⁹ Y	7.5	3.8
¹²⁴ Te	4.7	2.2
¹³⁶ Ba	4.1	2.2
¹³⁸ Ba	2.5	1.2
¹³⁹ La	1.7	0.8
¹⁵⁰ Sm	2.8	0.9
¹⁵¹ Eu	0.2	0.06
²⁰⁴ Pb	2.5	0.9
²⁰⁸ Pb	1.2	0.4

^aLow-mass AGB stars (LMS-AGB).

^bIntermediate-mass AGB stars (IMS-AGB).

the choice of the specific stellar evolutionary code. To this one may add the uncertainties connected with the treatment of the Galactic chemical evolution model. Among the most important uncertainties is the evaluation of the global ejecta from the AGB winds of stars of different masses and metallicities, which in turn depend on the mass mixed with the envelope by the various third dredge up episodes, and by the the weighted average *s*-process yields over the assumed ¹³C-pocket efficiencies. This would provide a very poor expectation. However, a strong constraint is given by the heavy *s*-only isotopes, whose solar abundance derives entirely from the *s* process in AGB stars. Among the *s*-only isotopes, the unbranched ¹⁵⁰Sm, whose neutron capture cross section at astrophysical temperatures and solar abundance are very well known, with a total uncertainty of less than 3% (Arlandini et al. 1999), may be chosen as normalisation. One may then deduce the relative *s*-process isotope percentage for all heavy elements.

For LMS we averaged the *s*-process yields over 13 ¹³C-pocket, excluding the case ST \times 2. For IMS, the effect of the ¹³C neutron source is negligible with respect to the one induced by ²²Ne neutron source.

In Table 1 we show values of AGB percentage to solar abundance at $t=t_{\odot}$ for LMS and IMS respectively obtained by present calculations compared with Travaglio et al. (1999) results. In Table 1 a choice of selected isotopes is made, among which the *s*-only isotopes ¹²⁴Te, ¹³⁶Ba, ¹⁵⁰Sm, and ²⁰⁴Pb, together with ⁸⁹Y, ¹³⁸Ba, and ²⁰⁸Pb of major *s*-process contribution. In turn ¹⁵¹Eu is chosen as representative of the *r* process, as clearly indicated by its only 6% to solar ¹⁵¹Eu.

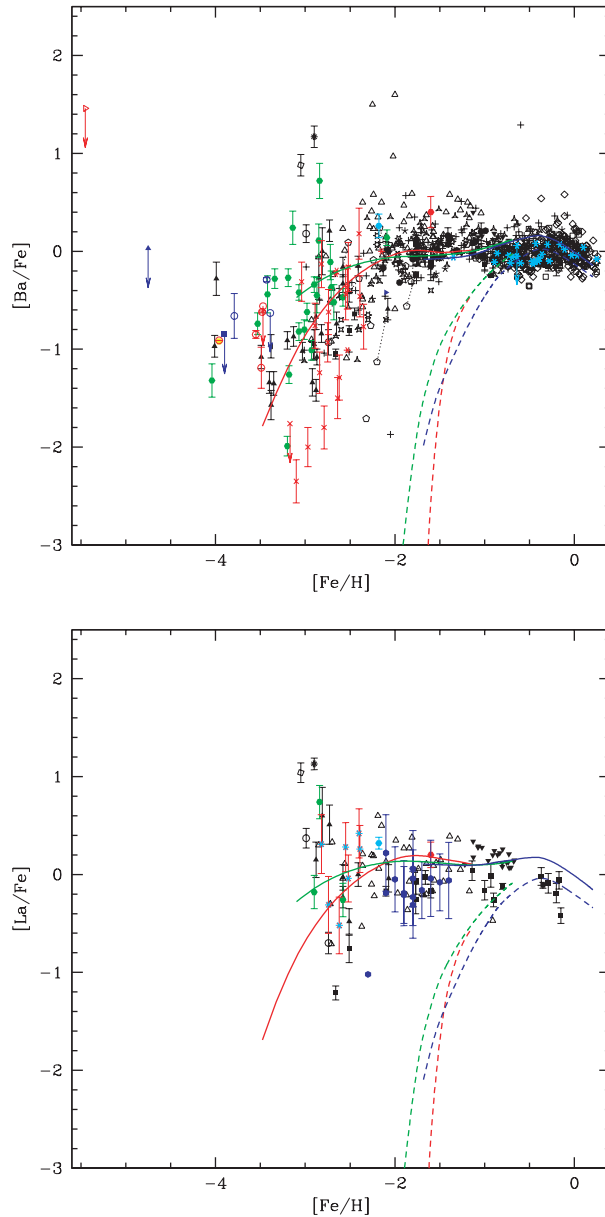


Figure 3 Top panel: evolution of [Ba/Fe] *s* fraction as function of [Fe/H] in the halo, thick disc, and thin disc are shown as dashed lines. Solid lines are for the total *s* + *r* Ba theoretical expectations. Spectroscopic observations of Galactic disc and halo stars for [Ba/Fe] versus [Fe/H] from literature (Travaglio et al. 1999, implemented with more recent observations as detailed in the text). Error bars are shown only when reported for single objects by the authors. The dotted line connects a star observed by different authors. Bottom panel: analogous plot for [La/Fe].

We compare our results with spectroscopic abundances of [Sr,Y,Zr/Fe], [Ba,La/Fe], and [Pb/Fe] that are typical of the *s*-process peaks, as well as [Eu/Fe], which in turn is a typical *r*-process element.

Let us first consider [Ba/Fe] and [La/Fe] versus [Fe/H]. Figure 3 shows in the top panel the [Ba/Fe] versus [Fe/H] with spectroscopic observations and theoretical *s*-curves, and in the bottom panel the analogous plot [La/Fe] versus [Fe/H]. In this figure, and the following, we compare with the set of stellar observations used by Travaglio

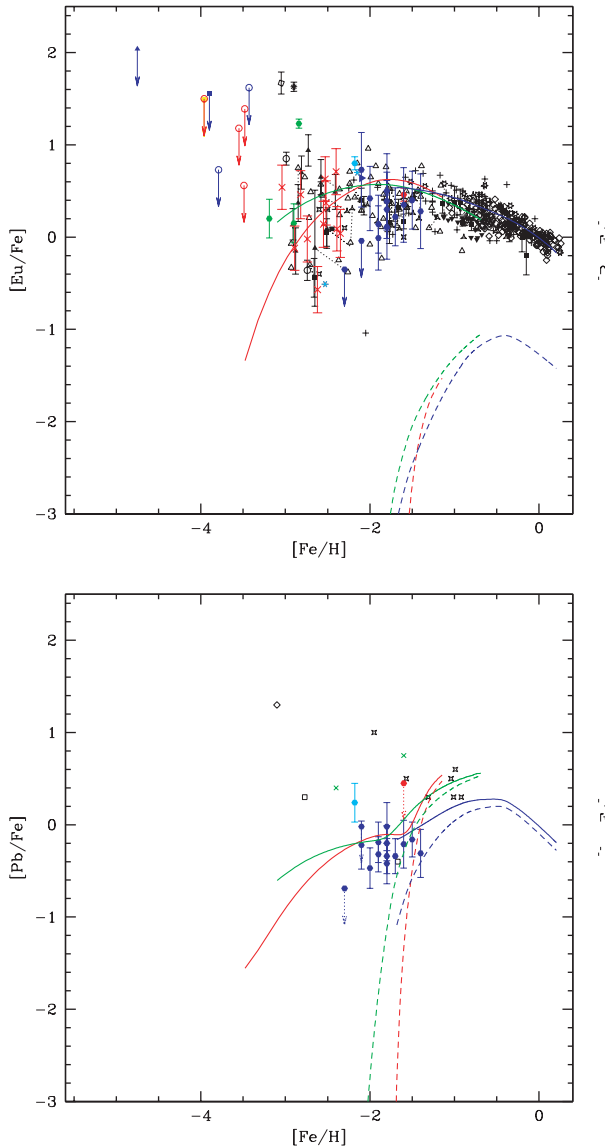


Figure 4 Top panel: Galactic chemical evolution of $[{\rm Eu}/{\rm Fe}]$ versus $[{\rm Fe}/{\rm H}]$ compared with spectroscopic observations. Bottom panel: analogous plot for $[{\rm Pb}/{\rm Fe}]$ versus $[{\rm Fe}/{\rm H}]$.

et al. (1999, 2001, 2004) implemented with more recent observations of elemental abundances in field stars, as listed below, with their associated symbols in the figures: Mashonkina & Zao (2006) blue asterisks; Ivans et al. (2006) cyan full hexagons; Aoki et al. (2008) red open squares; Aoki & Honda (2008) blue asterisks; Lai et al. (2008) green full hexagons; Cohen et al. (2007) yellow full hexagons; Norris et al. (2007) blue full triangles; Frebel et al. (2007) full blue squares; Mashonkina et al. (2008) red asterisks; Roederer et al. (2008) full red hexagons; Aoki et al. (2005) red crosses; François et al. (2007) cyan asterisks; Cohen et al. (2008) red open circles; Aoki et al. (2006) red open triangles pointing to the right; Yushchenko et al. (2005) blue full triangles; Van Eck et al. (2003) black open triangles; Cowan et al. (2002) green crosses. The dashed lines show the theoretical GCE expectations using only the AGB *s*-process products for halo, thick, and thin disc

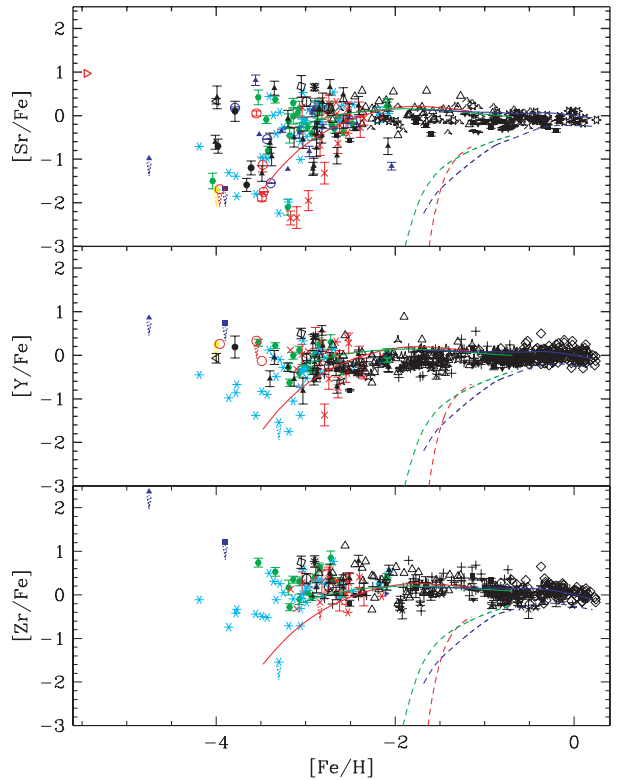


Figure 5 Galactic chemical evolution of $[{\rm Sr}/{\rm Fe}]$ versus $[{\rm Fe}/{\rm H}]$ (upper panel), $[{\rm Sr}/{\rm Fe}]$ versus $[{\rm Fe}/{\rm H}]$ (middle panel), and $[{\rm Zr}/{\rm Fe}]$ versus $[{\rm Fe}/{\rm H}]$ (lower panel) compared with spectroscopic observations.

separately. Although the *s* contributions to solar Ba and La are 78.2% and 66.3%, respectively, it is clear that *s* process alone does not explain all spectroscopic observations.

In Figure 4 analogous plots are shown for $[{\rm Eu}/{\rm Fe}]$ (top panel) and $[{\rm Pb}/{\rm Fe}]$ (bottom panel) versus $[{\rm Fe}/{\rm H}]$. While the *s*-process contribution to Eu is negligible (5.6% to solar Eu), the *s* contribution to solar Pb is 83.9%. Comparing with previous plots, spectroscopic $[{\rm Pb}/{\rm Fe}]$ observations are scarce because of the difficulty to extract Pb abundances from unevolved stars. As we explained before, the classical analysis of the main component cannot explain the $^{208}{\rm Pb}$ abundances. The GCE calculation provide 83.9% to solar Pb, and 91.1% to $^{208}{\rm Pb}$, thanks to the contribution of different generations of AGB stars. In particular, low metallicities AGB stars are the main contributors to $^{208}{\rm Pb}$.

Finally, in Figure 5 are presented the analogous plots for $[{\rm Sr}/{\rm Fe}]$ versus $[{\rm Fe}/{\rm H}]$ (top panel), $[{\rm Y}/{\rm Fe}]$ versus $[{\rm Fe}/{\rm H}]$ (middle panel), and $[{\rm Zr}/{\rm Fe}]$ versus $[{\rm Fe}/{\rm H}]$ (lower panel). GCE calculations provide 64.1% to solar Sr, 66.5% to solar Y, and 60.3% to solar Zr. Note that the classical analysis of the main component would provide 85%, 92%, and 83%, respectively (Arlandini et al. 1999), making clear also in this case that the classical analysis is only a rough approximation.

4.2 *r*-Process Yields and GCE

From the theoretical point of view, the *r*-process origin is still a matter of debate. The analytical approach followed

here to derive the *r*-process yields has been presented first by Travaglio et al. (1999). The enrichment of *r*-process elements in the interstellar medium (ISM) during the evolution of the Galaxy is quantitatively constrained on the basis of the results for the *s*-process contribution at $t = t_{\odot}$. The so called *r*-process residual for each isotope is obtained by subtracting the corresponding *s*-process contribution N_s/N_{\odot} from the fractional abundances in the solar system taken from Anders & Grevesse (1989):

$$\frac{N_s}{N_{\odot}} = \frac{N_{\odot} - N_s}{N_{\odot}} \quad (1)$$

In the case of Ba Travaglio et al. (1999) obtain a *r* residual of 21%. The assumption that the *r* process is of primary nature and originates from massive stars allows us to estimate the contribution of this process during the evolution of the Galaxy. In the case of Ba, for example

$$\left(\frac{\text{Ba}}{\text{O}}\right)_{r,\odot} \sim 0.21 \left(\frac{\text{Ba}}{\text{O}}\right)_{\odot} \quad (2)$$

Since the *s* process does not contribute at low metallicity for Population II stars

$$\left(\frac{\text{Ba}}{\text{O}}\right) \sim \left(\frac{\text{Ba}}{\text{O}}\right)_{r,\odot} \quad (3)$$

assuming a typical $[\text{O}/\text{Fe}] \sim 0.6$ dex for Population II stars. Thus, the *r*-process contribution for $[\text{Fe}/\text{H}] \leq -1.5$ dominates over the *s* contribution and roughly reproduces the observed values.

The procedure followed to extrapolate the *r*-process yields is independent of the chemical evolution model adopted and has been described in Section 2. The solution shown in the plots adopts SNI Ie in the mass range $8 \leq M/M_{\odot} \leq 10$ as primary producers of *r* nuclei. The [element/Fe] ratios provide information about the enrichment relative to Fe in the three Galactic zones, making clear that a delay in the *r*-process production with respect to Fe is needed in order to match the spectroscopic data at $[\text{Fe}/\text{H}] \leq -2$. The observations show that [Ba/Fe] begin to decline in metal-poor stars and this trend can be naturally explained by the finite lifetimes of stars at the lower end of the adopted mass range: massive stars in the early times of evolution of the Galaxy evolve quickly, ending as SNII producing O and Fe. Later, less massive stars explode as SNII, producing *r*-process elements and causing the sudden increase in [element/Fe]. At $[\text{Fe}/\text{H}] \sim -1$ halo stars, thick disc stars, and thin disc stars are mixed up.

The large scatter observed in [Ba/Fe], [La/Fe], and in [Eu/Fe] in halo stars can be ascribed to an incomplete mixing in the Galactic halo. This allows the formation of very metal-poor stars strongly enriched in *r*-process elements, like CS 22892-052 (Sneden 2000a). This star, with $[\text{Fe}/\text{H}] \sim -3.1$, shows *r*-process enhancements of 40 times the solar value ($[\text{Eu}/\text{Fe}] \sim +1.7$), and $[\text{Ba}/\text{Fe}] \sim +0.9$. Nevertheless its [Ba/Eu] is in agreement with the typical *r*-process ratios.

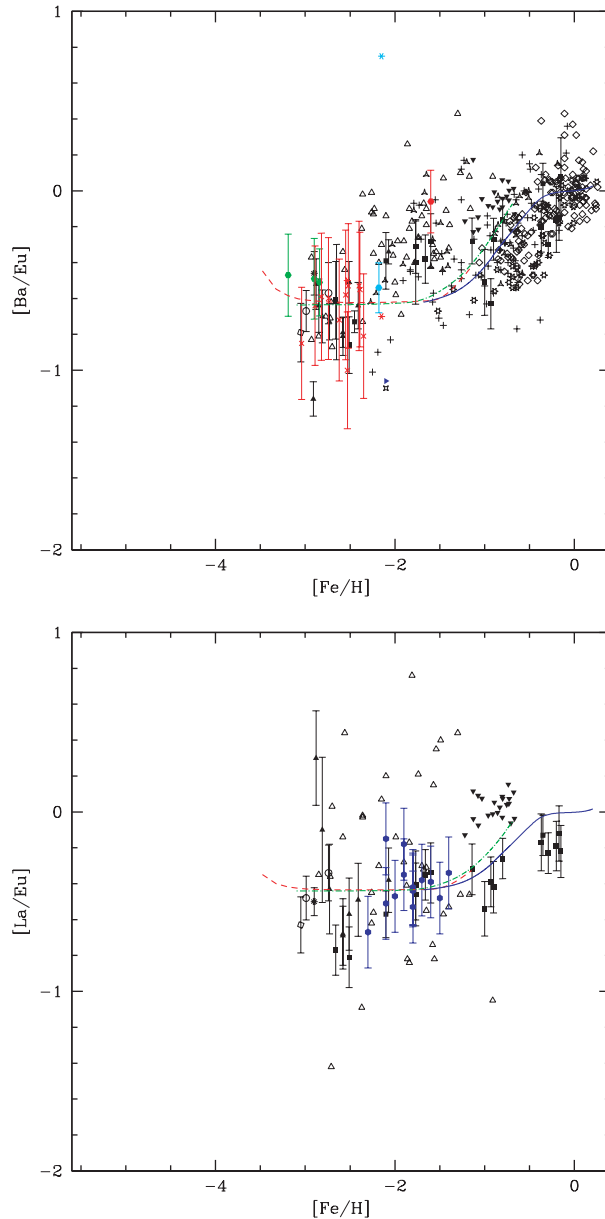


Figure 6 Top panel: Galactic chemical evolution of [Ba/Eu] versus [Fe/H] including both *s*- and *r*-process contributions in the thin disc (long-dashed line), thick disc (dotted line), and halo (solid line). Error bars are shown only when reported by the authors. Bottom panel: analogous plot for [La/Eu] versus [Fe/H].

4.3 Evolution of the *s* + *r* Process

The global results for the Galactic chemical evolution of heavy elements from iron to lead based on the assumptions discussed before, namely that the *s*-process contribution of these elements derives from low mass AGB stars and the *r*-process contribution originates from SNII in the range $8 \leq M/M_{\odot} \leq 10$, are shown as solid lines in Figures 3, 4, 5.

Figure 6 shows [Ba/Eu] versus [Fe/H] (top panel) and [La/Eu] versus [Fe/H] (bottom panel) for spectroscopic observations and theoretical curves computed by adding the *s*-and *r*-process contribution. Since Eu is mostly produced by *r*-process nucleosynthesis (94% at $t = t_{\odot}$), the

[element/Eu] abundance ratios (bottom panel) provide a direct way to judge the relative importance of the *s* and *r* channels during the evolution of the Galaxy. At low metallicity the *r*-process contribution is dominant, and the [element/Eu] ratio is given by the elemental *r* fraction computed with the *r* residuals described before. On the other hand, for $[\text{Fe}/\text{H}] \geq -1.5$, the *s*-process contribution takes over, and the [element/Fe] ratios rapidly increase approaching the solar values.

For elements from Ba to Pb, the estimated *r*-process contribution at $t = t_{\odot}$ has been derived by subtracting the *s* fraction from solar abundances (*r*-process-residual method). Instead, for elements lighter than Ba a more complex treatment is needed. In particular for Sr, Y, and Zr, besides the *s*-process component, one has to consider three other components: the weak *s* component (which decreases linearly with the metallicity), the *r* component and the LEPP-component, which are both independent of metallicity (Travaglio et al. 2004). As reported above, the GCE contribution by AGB stars are 64.1% to solar Sr, 66.5% to solar Y, and 60.3% to solar Zr. The weak *s* process is estimated to contribute to 9% to solar Sr, 10% to solar Y, and 0% to solar Zr. This leaves for the LEPP component a contribution of 17.9% to solar Sr, 18.5% to solar Y, and 28.7% to solar Zr very close to Travaglio et al. (2004) expectations. The residual *r*-process contributions would then be 9% of Sr, 5% of Y, and 11% of Zr. Summing up all contributions, the solid lines shown in Figure 5 give a good explanation of spectroscopic data, both in the halo and in the Galactic disc. A refined analysis is difficult to determine and is still matter of debate.

5 Conclusions

We have studied the evolution of the heavy elements in the Galaxy, adopting a refined set of models for *s* processing in AGB stars of different metallicities and compared with observational constraints of unevolved field stars for Sr, Y, Zr, Ba, La, Eu, and Pb. In the first part stellar yields for *s*-process elements have been obtained with post-process calculations based on AGB models with different masses and metallicities, computed with FRANEC.

In the second part we have adopted a Galactic chemical evolution model in which the Galaxy has been divided into three zones (halo, thick disc, and thin disc), whose composition of stars, gas (atomic and molecular), and stellar remnants, is computed as a function of time up to the present epoch. Introducing as a first step in the GCE model the AGB *s* yields only, we have obtained the *s*-process enrichment of the Galaxy at the time of formation of the solar system. Major uncertainties connected with the AGB models, with the adopted average of the large spread of ^{13}C -pocket efficiencies, as well as of the basic parameters introduced in the CGE model are strongly alleviated once we normalise the *s*-process isotope abundances computed at the epoch of the solar formation to ^{150}Sm , an unbranched *s*-only isotope with both a well-determined solar abundance and neutron-capture cross section at astrophysical temperatures.

Assuming that the production of *r* nuclei is a primary process occurring in SNII of $8\text{--}10 M_{\odot}$, the *r* contribution to each nucleus has then been computed as the difference between its total solar abundance and its *s*-process abundance. Finally we compare our predictions with spectroscopic observations of the above listed elements along the life of the Galaxy.

Acknowledgments

We acknowledge the anonymous referees for their very useful comments. We thank Maria Lugaro for a very careful reading of the manuscript. Work supported by the Italian MIUR-PRIN 2006 Project ‘Final Phases of Stellar Evolution, Nucleosynthesis in Supernovae, AGB Stars, Planetary Nebulae’.

References

- Anders, E. & Grevesse, N., 1989, GeCoA, 53, 197
- Aoki, W. et al., 2005, ApJ, 632, 611
- Aoki, W. et al., 2006, ApJ, 639, 897
- Aoki, W. et al., 2008, ApJ, 678, 1351
- Aoki, W. & Honda, S., 2008, PASJ, 60, L7
- Arlandini, C., Käppeler, F., Wissak, K., Gallino, R., Lugaro, M., Busso, M. & Straniero, O., 1999, ApJ, 525, 886
- Bao, Z. K., Beer, H., Käppeler, F., Voss, F., Wissak, K. & Rauscher, T., 2000, ADNDT, 76, 70
- Bisterzo, S., Gallino, R., Straniero, O., Aoki, W., Ryan, S. & Beers, T. C., 2006, AIPC, 847, 368
- Busso, M., Gallino, R. & Wasserburg, G. J., 1999, ARA&A, 37, 239
- Busso, M., Gallino, R., Lambert, D. L., Travaglio, C. & Smith, V. V., 2001, ApJ, 557, 802
- Cescutti, G., François, P., Matteucci, F., Cayrel, R. & Spite, M., 2006, A&A, 448, 557
- Chiappini, C., Matteucci, F. & Gratton, R., 1997, ApJ, 477, 765
- Clayton, D. D. & Rassbach, M. E., 1967, ApJ, 148, 69
- Cohen, J. G., McWilliam, A., Christlieb, N., Shectman, S., Thompson, I., Melendez, J., Wisotzki, L. & Reimers, D., 2007, ApJ, 659, L161
- Cohen, J. G., Christlieb, N., McWilliam, A., Shectman, S., Thompson, I., Melendez, J., Wisotzki, L. & Reimers, D., 2008, ApJ, 672, 320
- Cowan, J. J. et al., 2002, ApJ, 572, 861
- Ferrini, F., Matteucci, F., Pardi, C. & Penco, U., 1992, ApJ, 387, 138
- François, P. et al., 2007, A&A, 476, 935
- Frebel, A., Norris, J. E., Aoki, W., Honda, S., Bessell, M. S., Takada-Hidai, M., Beers, T. C. & Christlieb, N., 2007, ApJ, 658, 534
- Gallino, R., Arlandini, C., Busso, M., Lugaro, M., Travaglio, C., Straniero, O., Chieffi, A. & Limongi, M., 1998, ApJ, 497, 388
- Iben, I., Jr., 1975, ApJ, 196, 525
- Ivans, I. I., Simmerer, J., Sneden, C., Lawler, J., Cowan, J., Gallino, R. & Bisterzo, S., 2006, ApJ, 645, 613
- Käppeler, F., Beer, H., Wissak, K., Clayton, D. D., Macklin, R. L. & Ward, R. A., 1982, ApJ, 257, 821
- Lai, D. K., Bolte, M., Johnson, J. A., Lucatello, S., Heger, A. & Woosley, S. E., 2008, ApJ, 681, 1524
- Mashonkina, L. & Zhao, G., 2006, A&A, 456, 313
- Mashonkina, L. et al., 2008, A&A, 478, 529
- Matteucci, F., 2003, ASSL, 253
- Norris, J. E., Christlieb, N., Korn, A. J., Eriksson, K., Bessell, M. S., Beers, T. C., Wisotzki, L. & Reimers, D., 2007, ApJ, 670, 774
- Pagel, B. E. J., 1997, Nucleosynthesis and Chemical Evolution of Galaxies (Cambridge University Press)
- Pardi, M. C., Ferrini, F. & Matteucci, F., 1995, ApJ, 444, 207
- Roederer, I. U., Lawler, J. E., Sneden, C., Cowan, J. J., Sobeck, J. & Pilachowski, C. A., 2008, ASPC, 393, 263

- Sneden, C., Cowan, J. J. & Gallino, R., 2008, *ARA&A*, 46, 241
Straniero, O., Domínguez, I., Abia, C., Limongi, M. & Chieffi, A.,
2001, *MmSAI*, 72, 265
Straniero, O., Domínguez, I., Cristallo, S. & Gallino, R., 2003,
PASA, 20, 389
Travaglio, C., Galli, D., Gallino, R., Busso, M., Ferrini, F. &
Straniero, O., 1999, *ApJ*, 521, 691
Travaglio, C., Gallino, R., Busso, M. & Gratton, R., 2001, *ApJ*,
549, 346
Travaglio, C., Gallino, R., Arnone, E., Cowan, J., Jordan, F. &
Sneden, C., 2004, *ApJ*, 601, 864
Truran, J. W. & Iben, I., Jr., 1977, *ApJ*, 216, 797
Vaglio, P. et al., 1999, in *Nuclei in the Cosmos V*, Ed. Prantzos, N.
(Paris, Edition Frontières), 223
Van Eck, S., Goriely, S., Jorissen, A. & Plez, B., 2003, *A&A*, 404,
291
Wyse, R. F. G. & Gilmore, G., 1992, *AJ*, 104, 144
Yushchenko, A. et al., 2005, *A&A*, 430, 255